ORIGINAL RESEARCH ARTICLE

Effect of Preheating Temperature on Microstructure and Mechanical Properties of Friction Stir Welded DMR249A HSLA Steel Joints

Seerangan Ragu Nathan[1] · Visvalingam Balasubramanian[2] · Ardula Gourav Rao[3] · Tushar Sonar[4] · Mikhail Ivanov[4]

Abstract

The purpose of this research is to examine the influence of temperature of preheating on mechanical performance and microstructure of FSW joints of DMR249A steel. The FSW joints were produced with no preheating and preheating at 100, 150, 200 and 250 °C respectively. Tensile properties and toughness of FSW joints were reduced when the temperature of preheating was raised from 100 to 250 °C. This is primarily related to an increased input of heat that results in inclusions of tungsten due to the wear of W99 tool and grain coarsening in stir zone (SZ) of FSW joints. The FSW joints produced with no preheating and preheating at 100 °C displayed greater tensile properties and toughness compared to the FSW joints produced with preheating at 150, 200 and 250 °C. This refers to the greater refinement of SZ microstructure of FSW joints which is made up of greater bainite regions and acicular ferrite.

Keywords DMR249A microalloyed steel · Lanthanated tungsten alloy tool · Friction stir welding · Preheating · Microstructure · Mechanical properties

Introduction

In India, the DMRL (Defence Metallurgical Research Laboratory) has developed DMR249A steel which belongs to a domestic naval grade microalloyed (MA) steel also referred to as high-strength low-alloy (HSLA) steel. It has been employed to build the lightweight structures of aircraft carriers and modern ships. At temperatures as low as −60 °C, this type of steel exhibits exceptional toughness and higher strength. This lower-carbon (usually 0.08 weight percent) MA steel is manufactured by mixing in 0.03–0.05 weight percent V, < 0.05 weight percent Nb and 0.01–0.06 weight percent Ti. It is intended to develop a structure that is mostly ferritic and contains fewer than 10 volume % of pearlites [1]. This steel displays a greater strength/weight ratio, good combination of superior tensile properties and toughness at room and lower temperatures. Also, the weldability of DMR249A-MA steel is good [2]. Hence, it has evolved as the preferential grade of microalloyed steel for minimizing the weight of structures, pipes, storage tanks and pressure vessels in ships [3]. The DMR249A steel is primarily joined using fusion welding including SMAW (shielded metal arc welding) and GMAW (gas metal arc welding) processes. Hariprasath et al. [4] observed that the GMAW joints of DMR249A-MA steel exhibited 90.10% of fatigue strength of unwelded BM (base metal). The joint interface revealed the fatigue crack initiation that propagated in the HAZ (heat-affected zone). The evolution of residual stresses during welding which were tensile in nature were predominantly responsible for reduction in fatigue strength of GMAW joints. Pamnani et al. [5] suggested the usage of A-GTAW (activated flux GTAW) process for joining DMR249A-MA steel plates. The A-GTAW process exhibits lower cost and

✉ Seerangan Ragu Nathan
  ragucemajor@gmail.com

1   Micromachining Research Centre (MMRC), Department of Mechanical Engineering, School of Mechanical Engineering, Mohan Babu University (Erstwhile Sree Vidyanikethan Engineering College), Tirupati, Andhra Pradesh 517102, India

2   Centre for Materials Joining & Research (CEMAJOR), Department of Manufacturing Engineering, Annamalai University, Chidambaram, Tamil Nadu 608002, India

3   Naval Materials Research Laboratory (NMRL), Ambernath, Maharashtra 421506, India

4   Department of Welding Engineering, Institution of Engineering and Technology, South Ural State University (National Research University), Chelyabinsk 454080, Russia

enhanced productivity compared to SMAW process. The A-GTAW joints of DMR249A-MA steel showed 680 MPa tensile strength and 200 J impact toughness which are comparable to BM. The WM (weld metal) region displayed the development of acicular ferrite phases that contributes to the improved toughness of joints [6]. Mohammed et al. [7] reported 18.54 and 46.60% improved tensile strength and ductility of GTAW joints compared to SMAW joints. However, the resistance to stress corrosion cracking and pitting was superior in GTAW joints than SMAW joints. This relates to the higher martensitic phase development in WM of SMAW joints than GTAW joints. Hariprasath et al. [8] reported marginal 3.58% improved tensile strength for GMAW joints than SMAW joints as a result of enhanced refining of WM microstructure. The GMAW and SMAW joints failed in HAZ after tensile test. This corresponds to the reduced HAZ hardness than WM and BM region. Hariprasath et al. [9] observed marginal 2.92% improved fatigue strength of GMAW joints than SMAW joints. The fatigue strength of GMAW and SMAW joints is 355 and 342 MPa that corresponds to the 60 and 56% of tensile strength of unwelded BM. Venkateshkannan et al. [10] observed that the tensile properties of CW-GMAW (continuous wave-GMAW) and DP-GMAW (double pulse-GMAW) joints are comparable to BM. However, the DP-GMAW joints exhibited 9.36 and 34.92% enhancement in impact toughness than CW-GMAW joints at room temperature and at -60 °C respectively. The development of refine grains, higher % of acicular ferrite phases and high-angle grain boundaries in WM of DP-GMAW joints compared to CW-GMAW joints is mainly responsible for improved toughness of DP-GMAW joints.

Fusion welding of DMR249A-MA steel has certain issues. Welding thermal cycle and alloying contents both have an impact on fusion welding of MA steel. It changes the WM microstructure. The chances of H_2-induced cracking and lower hardness in HAZ make it more susceptible to fracture in HAZ region only. As a result, lower-H_2 ferritic steel filler wire can be utilized for welding MA steel [11]. The increased resistance against stress corrosion and H_2-assisted cracks in coarse-grained HAZ comprising martensite/austenite microstructure highlighted the importance of reducing the percentage of carbon in these kinds of steels [12]. In ship building applications, MA steel plates having a thickness from 3 to 40 mm are required and they must satisfy the requirements of good combination strength, ductility and toughness properties. The SMAW, GMAW and GTAW processes are effectively employed in shipbuilding industries for welding MA steel plates. However, these processes have the drawbacks of higher heat input owing to the increased number of welding passes that leads to the development of coarser WM microstructure and softened HAZ [10, 13]. This significantly deteriorates the strength and toughness of joints

and thereby adversely influences the service life of the shipbuilding structures. The framework parts of steel utilized in shipbuilding are welded together by panel lines. When part thickness falls below 13 mm, joint distortion develops significantly, increasing the cost of manufacturing and weld repairing operations [14].

Friction stir welding (FSW) is a cutting-edge solid state joining technique that has been employed for welding DMR249A-MA steel plates in order to solve these issues. FSW had been predominantly employed for welding aluminum alloys as of 1991 [15–20]. In FSW, the rotating tool developed with different profiles of pins such as conical, spherical, or threaded is employed. The tool material must be having higher hardness than the BM plates to be welded. The harder rotating FSW tool is plunged in and then traversed along the joint seam [21]. By not fusing metal plates together, FSW lessens the issues of hot cracks, porosity and distortion in welds that normally occur in fusion welding [22]. The rotating FSW tool plastically deforms the BM, and this stirring action modifies the coarser grain structure to finer grains [23]. FSW has proved to be a remarkably productive and sustainable welding process that eliminates radiation and harmful gases emitted from fusion welding. In comparison with traditional fusion welding, the positive aspects of FSW process additionally involve moderate residual stresses, minimal energy consumption and refined microstructure [24].

FSW has drawn a lot of research attention particularly when it pertains to joining metals with high fusion temperature notably titanium and steels owing to the technical advancements in tool material [25–30]. Ragu Nathan et al. [31] reported that the FSW joints of DMR249A-MA steel exhibited greater tensile properties and impact toughness at optimal tool rotational speed of 600 rpm. This relates to the development of refined acicular ferrite and upper bainite phases in microstructure of stir zone (SZ) without the debris of tool in SZ. The greater dynamic load impacting on the tool pin during plunging and increased BM dispersion into the tool pin results in inadequate plasticized flow of BM, caused significant deterioration of FSW tool. The 2.5 mm/min plunging rate of tool generated a sound joint devoid of defects and little tool wear [32]. Tiwari et al. [33] observed that the FSW joints of MA steel developed using ultrafine-grained WC tool exhibited 5 and 65% improvement in strength and hardness than the BM because of the evolution of Widmanstätten and acicular ferrite in SZ microstructure.

The severe welding conditions that come with FSW of hard metals may be more easily endured by these sophisticated tool materials. The simultaneous application of high flow stress and elevated welding temperatures (900 °C) during the FSW of steel can seriously deteriorate the tool. The following characteristics of a tool material have been shown by studies aimed at identifying appropriate tool

Fig. 1 Diagrammatic illustration of FSW with preheating sources
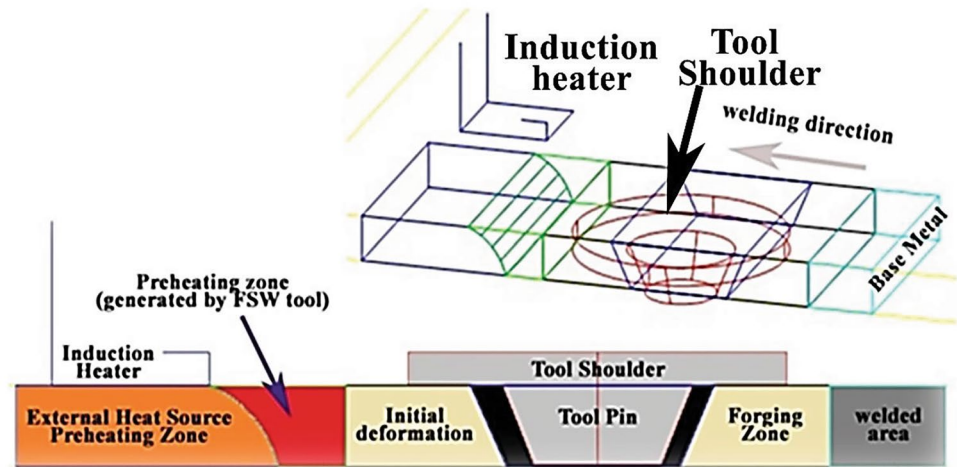
Table 1 Elemental contents (wt.%) of unwelded BM plates

V	Ni	Ti	Nb	Mo	W	Al	Cu	Si	N	Mn	C	Fe
0.032	0.69	0.016	0.035	0.02	0.04	0.032	0.126	0.19	0.015	1.42	0.08	Balance

materials for the FSW of steel: higher fracture toughness, superior yield strength at elevated temperatures, an impermeable microstructure, good wear resistance and inertness to the workpiece. Refractory-based alloys, particularly those based on tungsten (W), are one type of tool material that satisfies these criteria.

The tungsten (W)-based tools have yielded strong welds in titanium and steel alloys, but they undoubtedly increase the expense and complexity of the FSW procedure. Tool wear can be attributed to a combination of wear and tear or chemical affinity between the tool and base metal (BM) [34]. On the other hand, plastic deformation is linked to FSW generated variations in stress, strain rate and temperature. As a result, during the initial plunging phase, the pin experiences greater frictional and resultant forces, which the tool must bear [35, 36]. The strategies for reducing tool wear are as follows: (1) using high-red-hot hardness tool material; (2) tool profile and plunging rate optimization; (3) drilling a pilot hole in BM; and (4) positioning a preheating device in front of tool. In Fig. 1, the preheating of FSW joints is schematically represented. By developing the preheating area with an externally applied source of heat, it reveals the decrease in frictional and axial force on tool. Preheating is accomplished to minimize the wear on the tool because the pilot hole decreases the amount of stirring material. The starting BM temperature for the FSW is raised by figuring out additional techniques to heat the BM ahead of the tool. This lowers the amount of heat that the tool must supply, and consequently, the frictional forces.

Most of the research done on FSW welding of DMR249A-MA steel until now has been concentrated on GMAW, GTAW and SMAW processes. The existing study

**Table 2** Mechanical properties of unwelded BM plates

Tensile strength, MPa	0.2% offset yield strength, MPa	Elongation in 50 mm gauge length, %	Hardness, HV	Impact toughness, J
610	540	24	270	62

on FSW of DMR249A-MA steel is quite limited. The mechanical properties and microstructural evolution in different regions of FSW joints are strongly influenced by the temperature of preheating. It is crucial to comprehend the influence of temperature of preheating and degradation of W-based tool materials during FSW to progress the field and ensure the success in joining DMR249A-MA steel. The purpose of this research is to examine the influence of temperature of preheating (PHT) on mechanical performance and microstructure of FSW joints of microalloyed steel of DMR249A grade. The FSW joints were produced with no preheating and preheating at 100, 150, 200 and 250 °C respectively.

Experimental Details

Selection of Material and Joint Fabrication

The hot-rolled DMR249A-MA steel plates were received in the size of 150 × 350 × 5 mm. Tables 1 and 2 display the alloying elements and mechanical properties of unwelded BM plates. The microalloyed steel plates were joined employing FSW machine having the loading capacity of 60
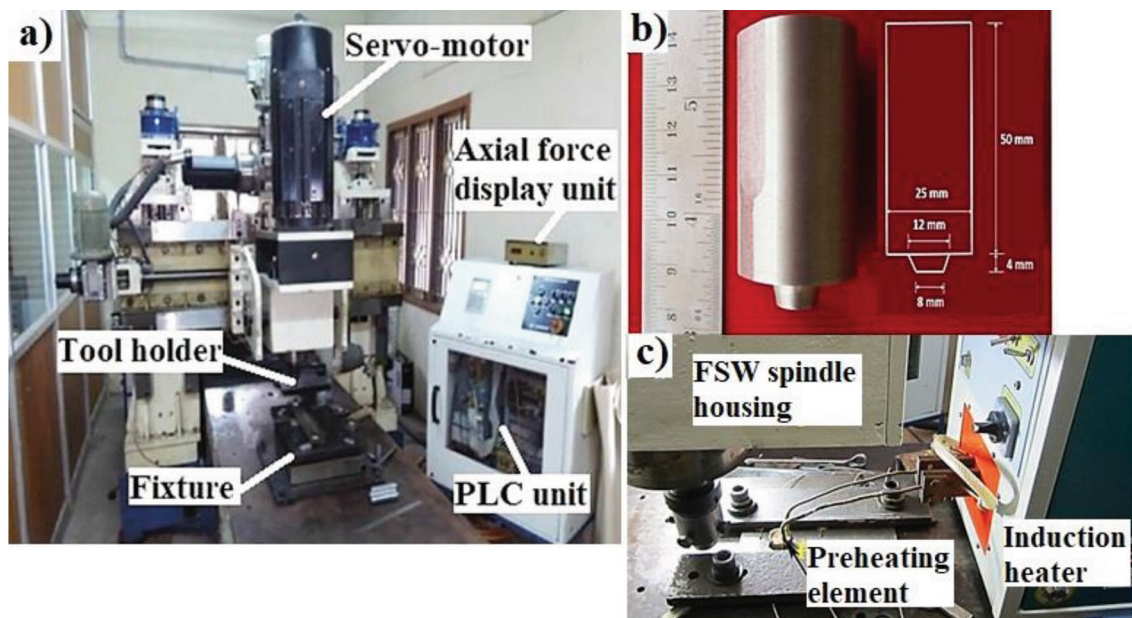
Fig. 2 Photograph of experimental setup: (**a**) FSW machine; (**b**) W99 tool; and (**c**) preheating induction heater

Table 3 Process parameters employed in fabricating the FSW joints of DMR249A-MA steel

Sr. No.	Process parameter	Value
1.	Temperature of preheating, °C	Without preheating, 100, 150, 200 and 250 °C
2.	Speed of tool rotation, rpm	600 rpm
3.	Speed of welding, mm/min	30 mm/min
4.	Plunge rate of tool, mm/min	2.5 mm/min

kN. The photograph of joint fabrication setup is displayed in Fig. 2a. The W99-tool was produced from tungsten alloy (W99) doped with 1% lanthanide oxide (La_2O_3). The W99-tool was manufactured through the route of powder metallurgy. The W99 tool and its dimensions are depicted in Fig. 2b. The joints were fabricated using the FSW parameters optimized by trial-and-error method. The FSW parameters employed for producing the joints are reported in Table 3. For temperature measurement, four thermocouples of K-type with a diameter of 1.0 mm were positioned on advancing side of BM, about 1.5 mm below the surface. The distance between the thermocouples and SZ center was 14 mm. The temperature was measured by wiring thermocouples into the first 6 data acquisition (DAQ) channels. Thermocouples had a DAQ device connected to it that could capture readings at 15 Hz. Readings were recorded using DAQ hardware that was in connection with a PC running software known as "LabVIEW." Figure 2c displays the experimental setup for measuring the temperature of preheating in FSW of BM plates. The FSW joints were fabricated at room temperature

(with no preheating), 100, 150, 200 and 250 °C. The processing range of preheating was set through trial and error by visually inspecting the joint defects and tool wear.

Microstructural Features

The metallographic specimens were cut from the fabricated FSW joints for the metallographic and microstructural studies. The cross section of the specimen was mirror polished utilizing different grades of emery papers and finer diamond polishing paste. The metallographic specimens were etched utilizing the standard etchant named "2% nital." The visual inspection of welds was analyzed using macrostructures of the FSW joints recorded using stereo zoom macroscope. The etched metallographic specimens were then analyzed under the optical microscope (OPM) and scanning electron microscope (SEM). The elemental analysis of SZ of FSW joints was studied using energy-dispersive spectroscopy (EDS). The electron backscatter diffraction (EBSD) technique was employed to study the orientation image mapping and grain boundary misorientation mapping of BM and SZ of FSW joint. The thin disk-shaped specimen having diameter of 3 mm was cut from SZ of FSW joint and ground mechanically to 100 μm thickness for microstructural analysis using transmission electron microscopy (TEM). The twin-jet electropolishing was performed on TEM specimens of SZ at − 10 °C and 22 V with a mixture of electrolyte consisting of 2% hydrofluoric acid, 3% nitric acid, 7% sulfuric acid, 10% lactic acid and 78% methanol.

Mechanical Testing

The transverse tensile specimens as per standard dimensions shown in Fig. 3a were cut from the FSW joints and marked with gauge length of 50 mm. Using a universal testing machine (UTM) rated with 100 kN loading capacity, the tensile test of FSW joints was carried out following ASTM E8M/8 standard. The subsized Charpy impact toughness specimens as per the standard dimensions shown in Fig. 3b were cut from the FSW joints and were machine with V-notch having an included angle of $45°$ and 2 mm depth. Using an impact toughness testing machine of pendulum type rated with 300 J capacity, the impact toughness of FSW joints was evaluated following ASTM E23 standard. The Vickers microhardness testing machine was employed to determine the microhardness distribution across the different regions of FSW joints. The microhardness was measured as per ASTM E347 standard using a polished and etched cross-sectional areas of metallographic specimens of FSW joints that were subjected to the indentation load of 500 g and dwell time of 15 s.

Results

Preheating Analysis

Figure 4 displays the photographs of the top view of FSW joints fabricated with no preheating and at different preheating temperatures. The FSW joint fabricated with preheating showed finer bead formation without flash. The FSW joint fabricated with preheating at 100 °C showed the formation of discontinuous ripples on weld surface. The FSW joint fabricated with preheating at 150 °C revealed the development of large amount of weld flash. An uneven shoulder influenced surface was observed when the FSW joints were fabricated at 200 °C. The sticking effect of BM to W99 tool was seen on the

weld surface of joints fabricated with preheating at 250 °C. Figure 5 displays the temperature distribution graphs for the FSW joints with no preheating and at different preheating levels. During the preheating stage, the temperature began to rise. The temperature of BM began to rise as the plunging phase of tool began, and it progressively reached its peak temperature at the ending phase of tool plunging. Different temperature peaks were attained at the end of plunging phase of tool because of preheating. As soon as the tool was removed from the BM, the temperature dropped. The preheating regulates not only the temperature induced by FSW parameters, but also the amount of heat supplied and peak temperature. Inconsistent high weld thermal cycles prior to and following the stirring action of W99 tool are responsible for the development of discontinuous weld and the emergence of more flash. Additionally, there is no indication of geometric defects and the sticking effect of BM on W99 tool is decreased with a reduction in preheating. The joints fabricated with no preheating showed the highest peak temperature of 1080 °C during FSW. As the temperature of preheating increased, the peak temperatures in BM during FSW were reduced to 550, 750, 800 and 650 °C, with preheating at 100, 150, 200 and 250 °C. The preheating area at leading edge of W99 tool needs to be kept consistent throughout the process to minimize the flow stress on W99 tool. That was obtained when the joints were produced with no preheating and with preheating at 100 °C. Therefore, it features a smooth surface devoid of surface defects and weld flash.

Macrostructures

The influence of the temperature of preheating on macrostructure of FSW joints is displayed in Table 4. All the FSW joints fabricated with no preheating and at different preheating temperatures of 100, 150, 200 and 250 °C were free from defects. The FSW joints showed full penetration

Fig. 3 Dimensions of (**a**) tensile and (**b**) Charpy impact toughness test specimen
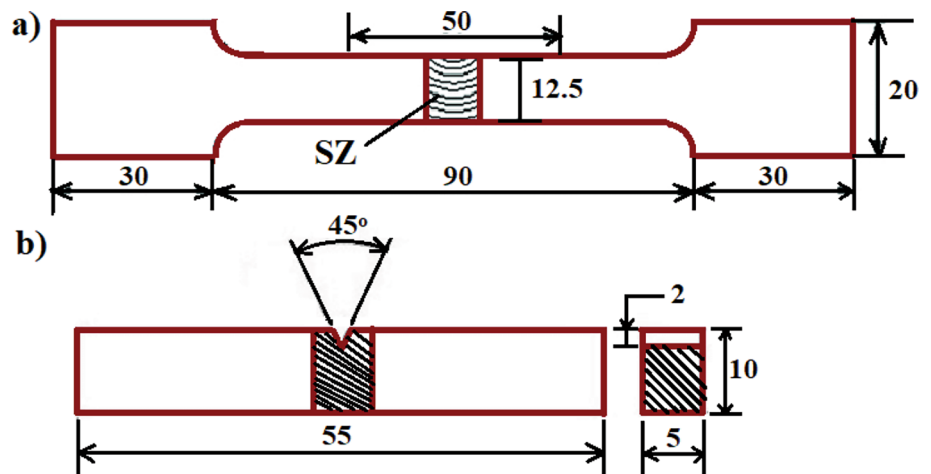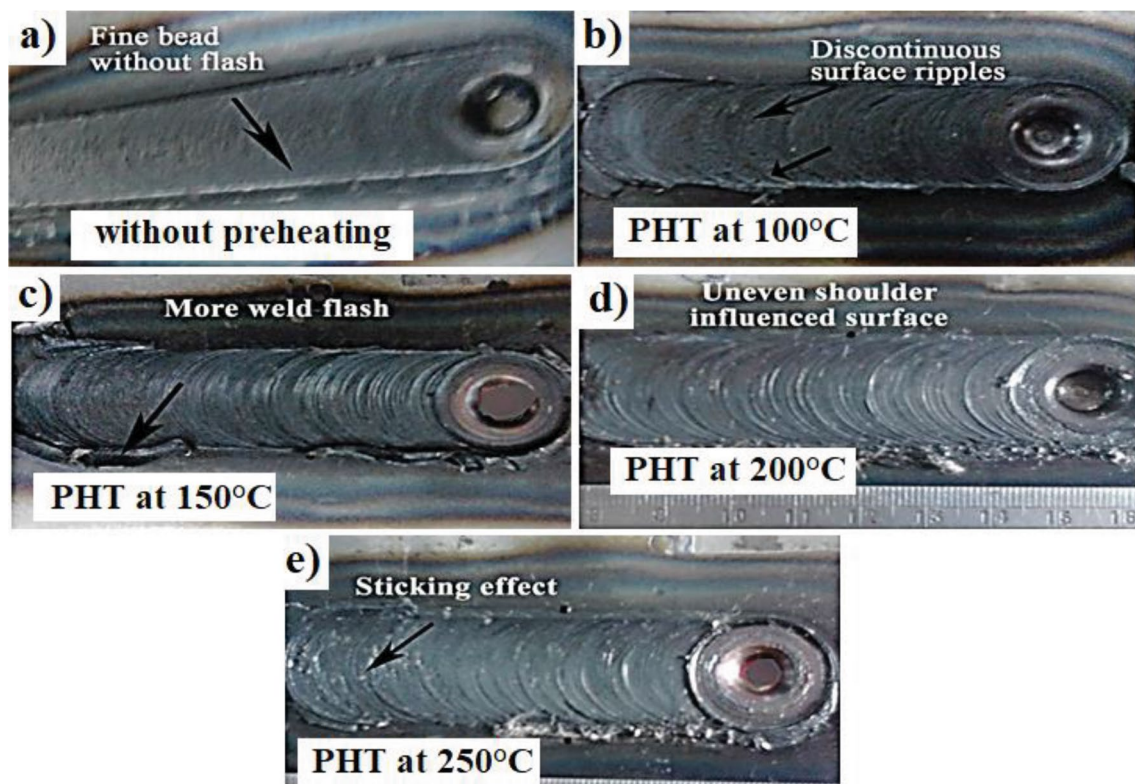
Fig. 4 Photographs of top view of FSW joint

and extreme frictional stirring of SZ. The SZ size was noticed to be the same in all the FSW joints. However, the FSW joints showed different width of HAZ when produced with no preheating and at different levels of preheating temperatures. As the temperature of preheating rises, the width of HAZ widens because heat dissipates in the BM long before the W99 tool approaches it. The FSW joint that was produced with no preheating has no defects and shows that there was enough stirring throughout the operation. On the other hand, the FSW joint that was produced with preheating at 100 °C showed that minimal material flow friction was induced by W99 tool damage from excessive heat dissipation. The macrographs show that the joints produced with preheating at 150, 200 and 250 °C had excessive flash development and improper flow pattern of material. That may be the result of unplasticized material flowing round the pin of the tool throughout the operation, which causes the tool pin to slide and stick. The FSW joint that was produced with no preheating and with preheating at 100 °C was determined to be free from defects that revealed no apparent debris of W99 tool.

Microstructure

The optical microstructure of BM and SZ of FSW joints fabricated with no preheating and at different preheating temperatures is depicted in Fig. 6. The microstructure of the BM comprises of ferrite, with traces of pearlite. Due to extreme plastic deformation, SZ has undergone a phase transition from ferrite to bainite. The FSW joints made with no preheating showed refined grain evolution in SZ without tool wear and need of preheating. It also shows that the most efficient generation of heat from the W99 tool for plasticizing the SZ is achieved with no preheating. SEM microstructures of BM and SZ of FSW joints produced with and with no preheating are displayed in Fig. 7. The SZ of the FSW joint produced with no preheating displays the bainitic structure and grain refinement. Oxides were found in the SZ microstructure of FSW joint, which was produced using preheating at 100 °C. The percentage of oxide in the microstructure of SZ of FSW joints increased when the temperature of preheating was raised from 150 to 250 °C. During FSW, preheating causes oxidation by providing localized heating to top surface of BM. The oxides in SZ can possibly be forged by the rubbing motion of the shoulder of the W99 tool. Therefore,

Fig. 5 Temperature distribution during fabrication of FSW joints at: (**a**) RT (with no preheating), (**b**) at 100 °C, (**c**) at 150 °C, (**d**) at 200 °C and (**e**) at 250 °C
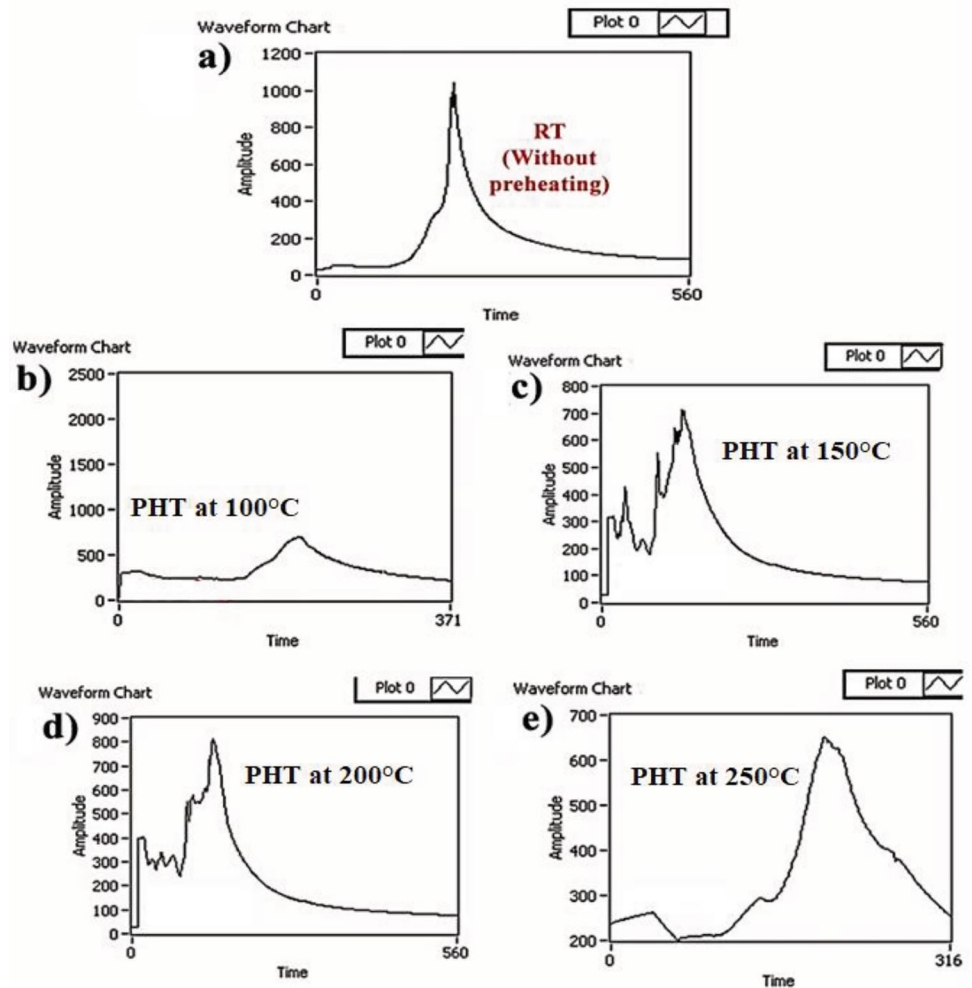
in comparison with a joint developed with no preheating, the additional localized heating may have an impact on the mechanical properties of FSW joints. Additionally, compared to the FSW joints developed with no preheating and with preheating at 100 °C, a progressive decrease in grain refinement was seen in the FSW joints made by making use of preheating at 150–250 °C. Entrapment of oxide particles in joints produced with preheating at 150–250 °C was confirmed by the EDS analysis, depicted in Fig. 8. Nevertheless, in FSW joints produced with no preheating and with preheating at 100 °C, the SZ microstructure free of oxides was seen.
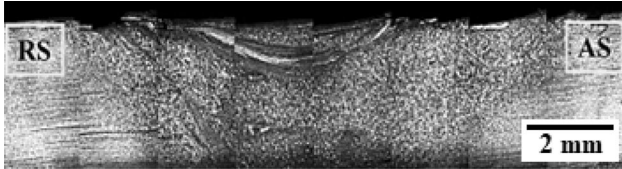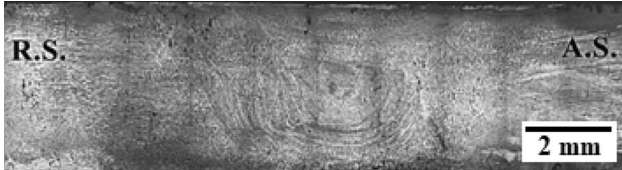
Figure 9 displays results of the EBSD analysis of BM and SZ of FSW joint that was made with no preheating. Figure 9a and 9b displays the boundary mapping and image quality of BM, separately. Figure 9c and 9d, respectively, displays the boundary mapping and image quality of SZ of FSW joint. It showed that there was greater refinement in the microstructure of SZ of FSW joint compared to BM.

Furthermore, compared to the BM, the SZ has greater high-angle grain boundaries (HAGBs), which are black in color. This could be the main reason for the superior mechanical properties of FSW joint than that of BM.

The misorientation of the boundaries and sizes of grains in the SZ of FSW joint is evident in Fig. 10. Micrographs revealed the presence of HAGBs and low-angle grain boundaries (LAGBs); nevertheless, Fig. 10a indicates the proportion of each, suggesting that the selected FSW parameters caused an adequate dynamic recrystallization of grains in SZ microstructure. Figure 10b displays the grain size evaluation of SZ of FSW joint made with no preheating. It reveals that the joint produced with no preheating fully realized the inherent characteristics of grain refinement and homogeneous microstructural development in SZ.

The SEM and TEM micrographs of SZ of FSW joint produced with no preheating are presented in Fig. 11. The SEM micrograph of SZ displayed the phases of finer lath ferrite and upper bainite. There were no inclusions of tungsten (W) in the SZ of joint. The TEM micrographs proved that in both low and high dislocation density areas, the BM was

Table 4 Influence of preheating on macrostructure of SZ

Preheating temperature	Macrostructure	Observations
With no preheating		Defect-free and refined SZ was observed
100 °C		Defect-free but severe deformation was observed
150 °C		Severe deformation and more heat dissipation was observed
200 °C		Reduced pin influenced region was observed
250 °C		Reduced pin influenced region was observed

appropriately integrated and homogenized without wear of the W99 tool. The EDS evaluation of W99 tool is shown in Fig. 12 both prior to and following the FSW. The EDS mapping results show a W-free SZ of FSW joint in Fig. 13.

Mechanical Properties

Table 5 displays the influence of the temperature of preheating on mechanical properties of FSW joints of DMR249A-MA steel. The BM exhibited the ultimate tensile strength (UTS) of 610 MPa, yield strength (YS) of 540 MPa, elongation of 24% and impact toughness (IT) of 62 J. The mechanical properties of FSW joints are inferior to the BM. However, the FSW joints produced with no preheating and with preheating at 100 °C showed higher UTS than the BM. The FSW joints produced with no preheating and with preheating at 100 °C displayed greater tensile properties and toughness compared to the FSW joints produced with preheating at 150, 200 and 250 °C. This refers to the greater refinement

of SZ microstructure of FSW joints. The FSW joints produced with no preheating showed the UTS of 664 MPa, YS of 502 MPa, El of 19% and IT of 48 J. Compared to BM, the UTS of FSW joint produced with no preheating was improved by 8.85% along with 7.03, 20.83 and 22.58% reduction in YS, EL and IT. The FSW joints produced with preheating at 100 °C showed UTS of 622 MPa, YS of 486 MPa, EL of 22% and IT of 49 J. Compared to BM, it revealed 1.96% improvement in TS along with 10, 8.33 and 20.96% reduction in YS, EL and IT. Tensile properties and toughness of FSW joints were reduced when the temperature of preheating was raised from 100 to 250 °C. This is primarily related to an increased input of heat that results in inclusions of tungsten due to the wear of W99 tool and grain coarsening in SZ of FSW joints.

The influence of preheating temperature on the microhardness distribution of FSW joints of DMR249A-MA steel is displayed in Fig. 14. The influence of preheating temperature on mean SZ microhardness of FSW joints is shown in Table 6. The 270 HV hardness was noticed in the BM. Since

Fig. 6 Optical microstructure of (**a**) BM and SZ of joints produced at (**b**) RT (with no preheating) and preheating at (**c**) 100 °C, (**d**) 150 °C, (**e**) 200 °C, (**f**) 250 °C
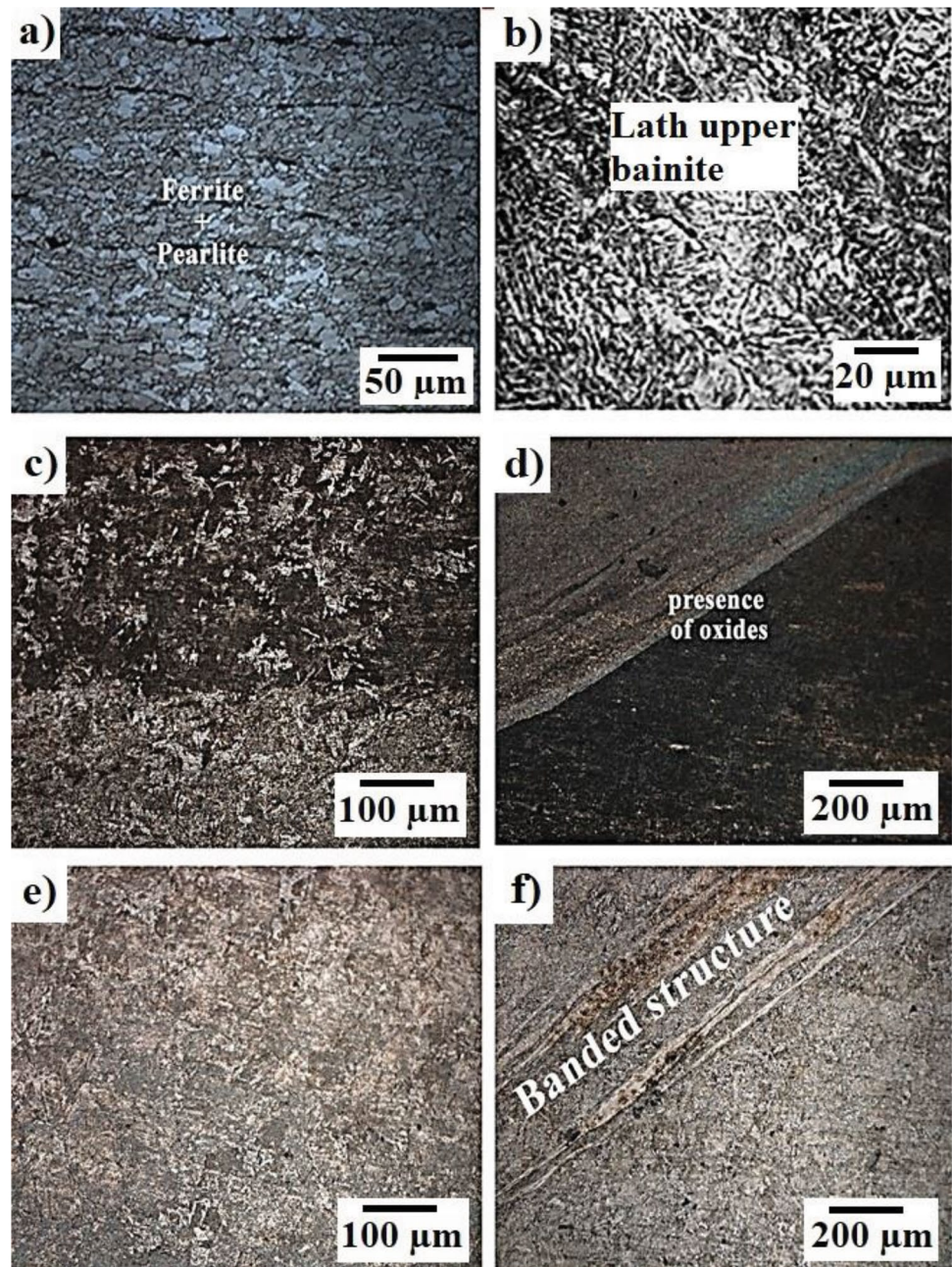
the material was stirred using a rotating W99 FSW tool, the finer grain structure evolved in SZ of all the joints, resulting in higher SZ hardness than BM. In comparison with BM and other joints produced at various preheating temperatures, the FSW joints produced with no preheating showed higher SZ hardness of 410 HV. When comparing hardness of SZ to BM, it revealed a 51.85% enhancement. The SZ hardness of FSW joints decreases with a rise in preheating temperature from 100 to 250 °C. This primarily relates to the increased input of heat that causes growth of grains in SZ microstructure of FSW joints. In comparison with FSW joints produced at different preheating temperatures, the joints produced with

preheating at 100 °C showed higher SZ hardness. The SZ hardness of 380 HV was found in the joints produced with preheating at 100 °C. In comparison with BM, it revealed a 40.74% enhancement in SZ hardness. Due to their lesser hardness than SZ and BM, the majority of the FSW joints on the advancing side HAZ (AS-HAZ) failed.

Fig. 7 SEM microstructure of (**a**) BM and SZ of joints produced (**b**) with no preheating and preheating at (**c**) 100 °C, (**d**) 150 °C, (**e**) 200 °C, (**f**) 250 °C
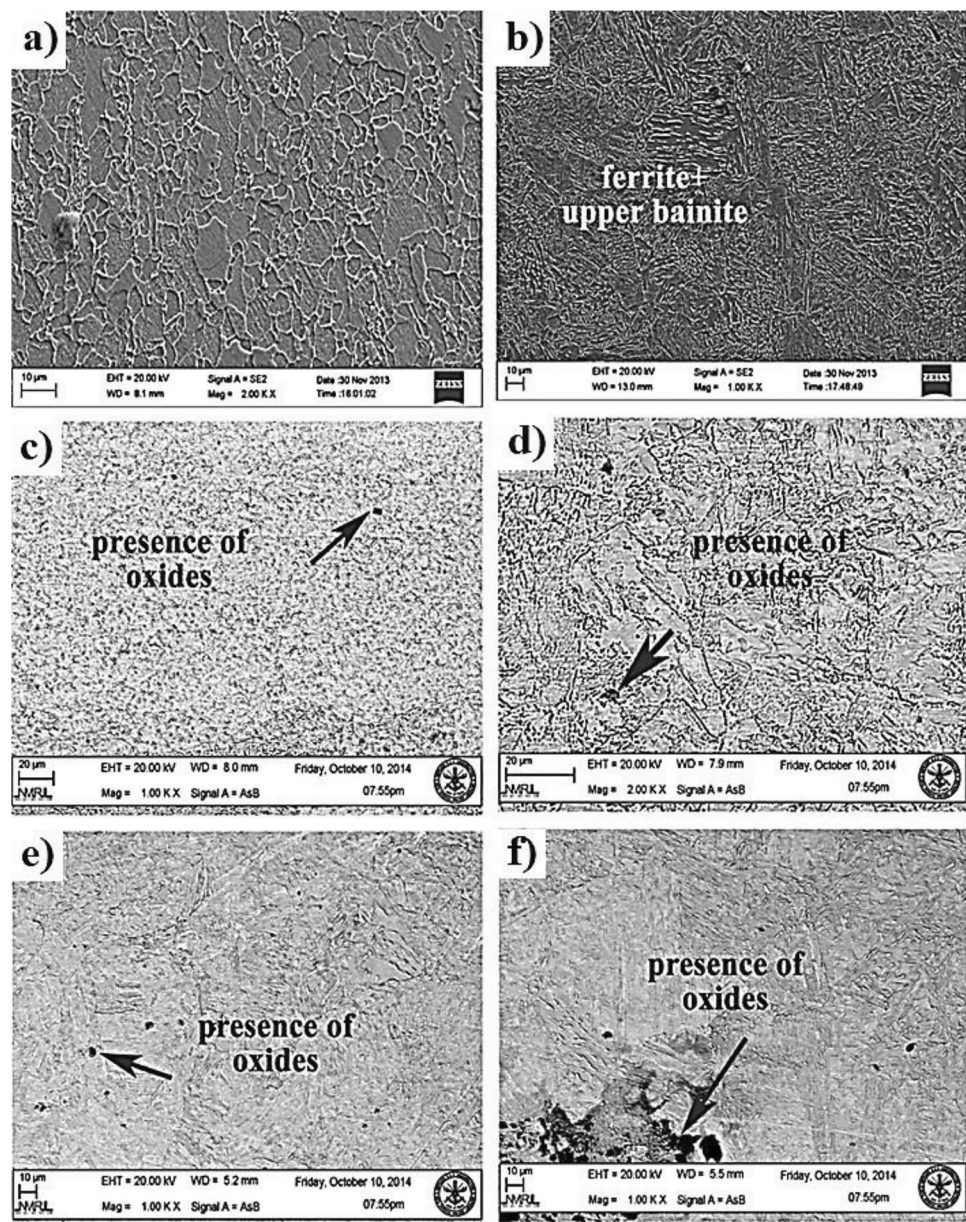
Discussion

The stresses and heat produced during FSW of DMR249A steel could be sustained by the W99 tool. The tool bends and wears due to greater flow stresses (force from BM to W99 tool), and the pin of tool particularly takes all the impacts during FSW rather than the shoulder of tool. There is a lot of ambiguity regarding the tool life and mechanical performance of FSW joints, despite the fact that the distortion and wear of tool aren't readily apparent in SZ [37]. The favorable material flow surrounding the pin of W99 tool can be accommodated by selecting a suitable design of tool and by considering the mechanical properties of BM. Welding temperatures and BM Flow stresses produced during frictional

stirring have an impact on the deterioration of tool in FSW of hard BMs [38]. The configuration of pin of the tool prior to plasticizing the BM should not be influenced by the action of an axial load at a given point in time. This may also have affected the tool material cost, quality of weld and life of tool. As a result, the process preheating was applied prior to the external source of heat (confined heating of BM) to lessen the axial load. Due to localized stress imposed by the increase in adherent torque, the tool pin broke [39]. Perhaps around the corners of W99 tool's pin, the stress concentration has grown. The compression caused by the vertical force is projected to diminish the matrix densification, and the forces generated by the BM will probably propagate the crack throughout the matrix phase of W99 tool. Using
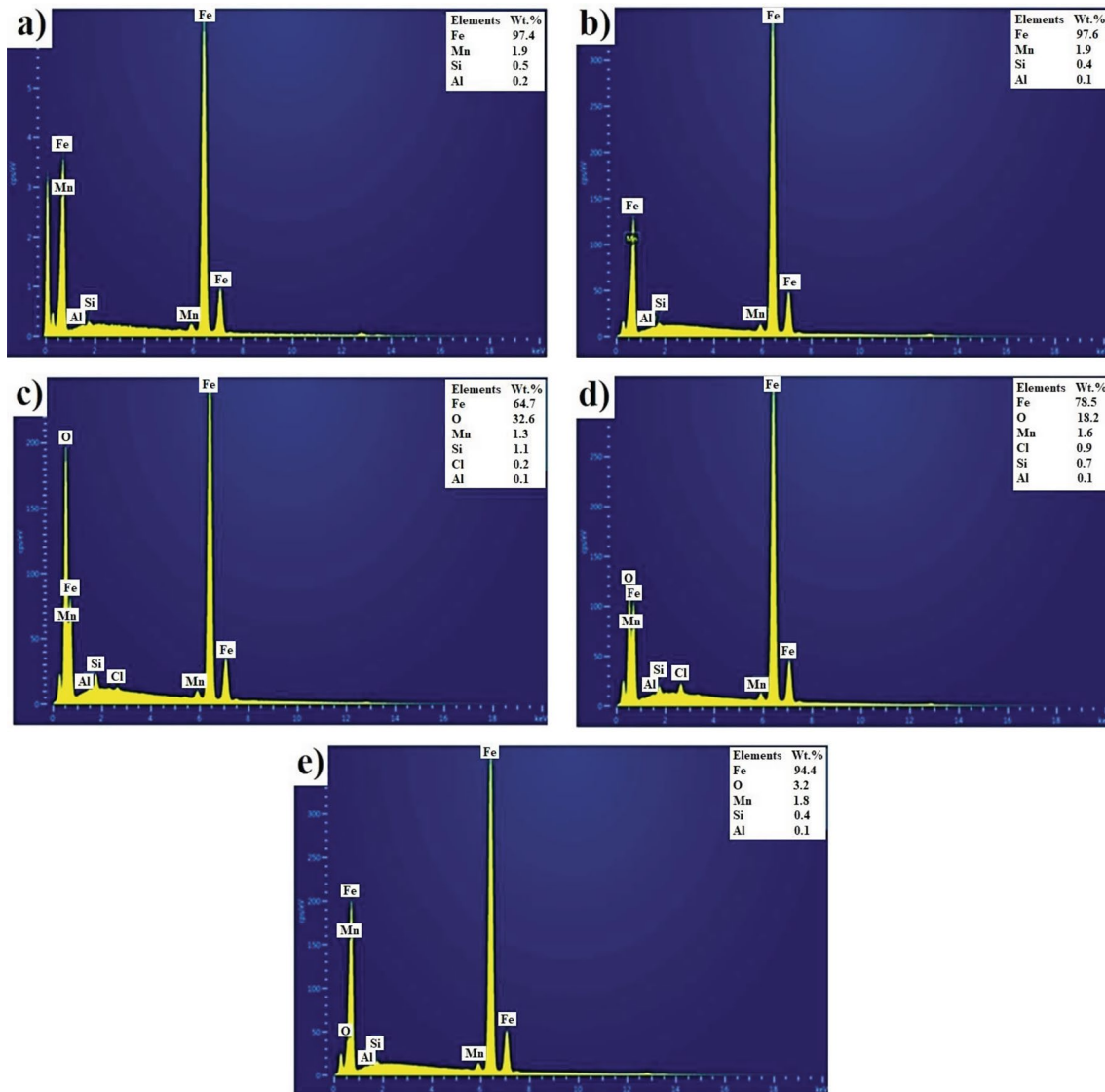
Fig. 8 EDS spectrum of SZ of FSW joints made at (**a**) RT (with no preheating) and preheating at (**b**) 100 °C; (**c**) 150 °C; (**d**) 200 °C; (**e**) 250 °C

the proper preheating temperature for welding DMR249A-MA steel plates enabled the elimination of this issue. This is mostly due to the decrease in vertical and consequent forces developed in FSW. Preheating is primarily recommended to reduce weld flash that may result from substantial frictional torque and axial force. Weld flash is higher in FSW joint produced with preheating temperature higher than 100 °C. Additionally, the material flow surrounding the pin of tool is significantly influenced by microstructural characteristic of joints developed with preheating. BM that has been heated by induction can become ductile shortly and can be readily integrated. The ductile characteristic of joints causes the SZ hardness to drop when the preheating temperature rises. The ductile nature of material controls the joint strength when subjected to elevated preheating

temperatures. The primary factor influencing the weld strength at lower temperature was material turbulent flow brought on by the churning motion of W99 tool [40]. Due to excessive preheating temperature, the material's turbulent flow clearly shows that there is significant heat generated in the SZ. The mechanical properties of FSW joints may be significantly influenced by the influence of induction preheating temperature on the dynamic recrystallization during FSW. With preheating at 100 °C, good welds that failed through ductile modes can be produced at very low load applied and rotational speed. With no preheating, frictional heat will be reduced in relation to FSW [41]. A portion of heat required to achieve good welds could be accounted for preheating. For FSW of hard BMs, preheating temperature must be controlled to prevent inconsistent temperature cycles.
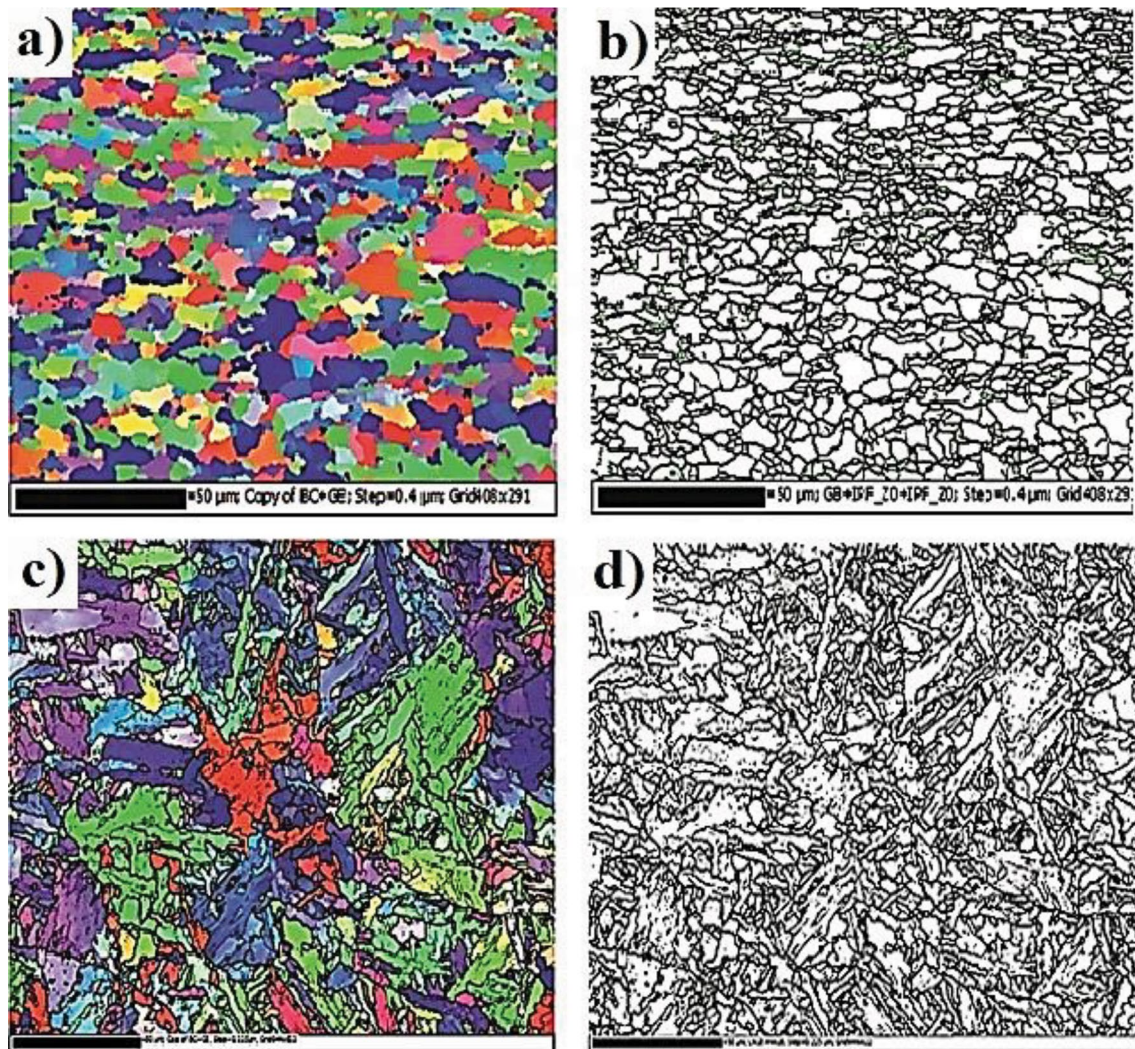
Fig. 9 EBSD micrographs: a) orientation image map and (**b**) grain boundary misorientation map of BM; (**c**) orientation image map and (**d**) grain boundary misorientation map of SZ of joint

The development of microstructure in SZ of joints is significantly influenced by the alloying compositions and frictional heat throughout FSW. Because of the slower rate of cooling caused by increased frictional heat, the SZ of FSW joints acquired a coarse-grained structure. Conversely, a faster rate of cooling induced by reduced frictional heat leads to the development of a fine-grained microstructure in SZ of FSW joints [42]. Reduced heat of friction may result in insufficient plasticized flow of material surrounding the pin of W99 tool, despite the fact it is desirable as it helps develop a fine-grained microstructure in SZ. Wear of tool increases as a consequence of increased flow stress on the pin of W99 tool. Increased heating also results in an irregular flow of material surrounding the pin of tool, promoting the development of excessive flash. Consequently, the FSW parameter and profile of the tool are crucial for producing welds free from defects. The fine-grained microstructure, primarily comprised of the upper bainite and acicular ferrite phases, is responsible for the enhanced strength of FSW joints. This occurs because, within massive austenite grains, the plates of acicular ferrite nucleate intragranularly on nonmetallic inclusions. From those inclusions, the plates extend in a variety of orientations while retaining an orientation related with the austenite [43]. In contrast to BM, the grain misorientation angle may be the primary factor in enhancing the yield and tensile strengths of joints. Because of the slower rate of cooling, all FSW joints with preheating exhibited the development of equiaxed grains with somewhat larger grain sizes in the microstructure of SZ [44]. In comparison with FSW joints with no preheating, the TMAZ of FSW joints with preheating had a lower percentage of HAGBs. This could potentially be the cause of FSW joint developed with no preheating achieving a higher strength than the joint produced with preheating.
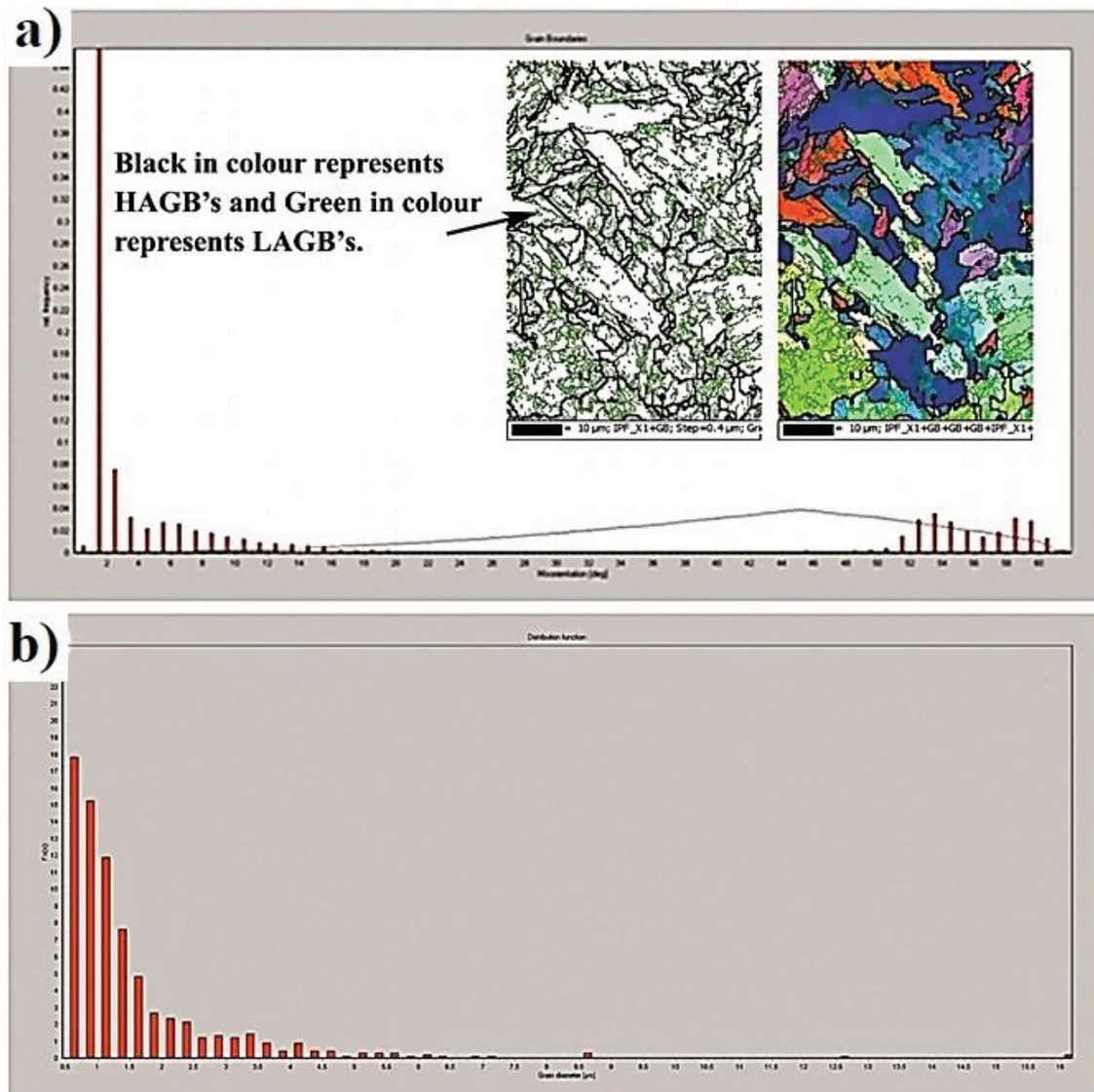
Fig. 10 EBSD results showing: (**a**) HAGBs and (**b**) grain size in SZ of FSW joint produced with no preheating

Furthermore, the fundamental factor that may be responsible for the undesirable mechanical characteristics obtained in joints produced employing preheating is the trapping of oxide particles. The joint produced with no preheating displayed HAGBs having misorientation angle ≥ 15° while the SZ microstructure disclosed finer ferrite and higher bainite. In comparison with the microstructure containing more HAGBs, Mehmet and Cemal [37] found that the microstructure of BM containing less HAGBs than the SZ of joint, indicates that the crack growth will occur more rapidly. Because of this, the breakage occurs in the AS-TMAZ as opposed to the AS-HAZ, which shows greater LAGBs. Grain refinement also occurred in the SZ under conditions of severe plastic deformation. Consequently, the size of grains in SZ was noticeably finer than BM. This reduction in grain

size lessens ductility while increasing joint strength [16, 25]**.** The process of dynamic recrystallization occurs during the flow of material in FSW. The increased joint strength is mostly attributable to fine-grained microstructure of SZ, which is made up of greater bainite regions and acicular ferrite. It results from the intragranular nucleation of acicular ferritic plates on nonmetallic impurities within the grains of austenite that are greater in size. The plates extended in several directions while maintaining an orientation contact with austenite [43]. The grain misorientation angle is crucial for enhancing the strength in relation to BM. At room temperature, the Charpy V-notch IT of BM is 62 J, whereas the IT of FSW joint shows 48 J, which is 38% less than that of BM. The IT of upper bainite is adversely affected by cementite thin layers at the lath boundaries of bainite because they

Fig. 11 (**a**) and (**c**) Macrostructure of cross-sectional area of FSW joint; SEM micrograph of SZ of FSW joint produced without preheating at (**a**) 500X magnification and (**b**) 5000X magnification; (**d**) TEM microstructure showing SZ without inclusions of tungsten particles from tool wear and e) TEM microstructure showing SZ high dislocation density
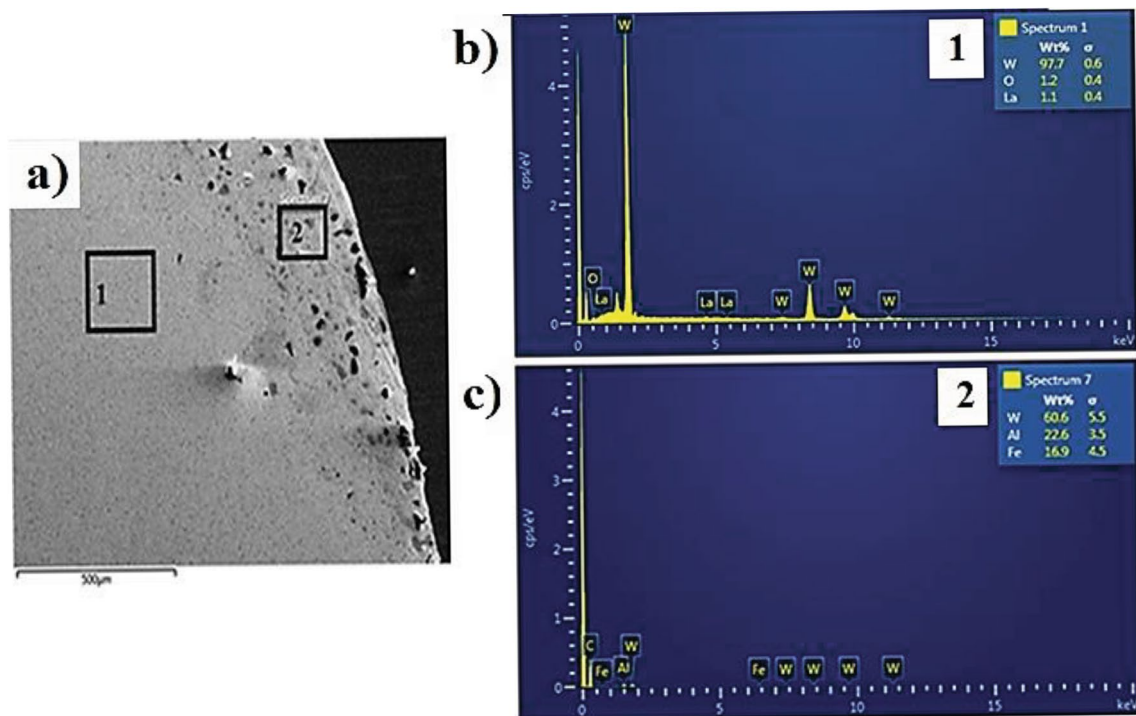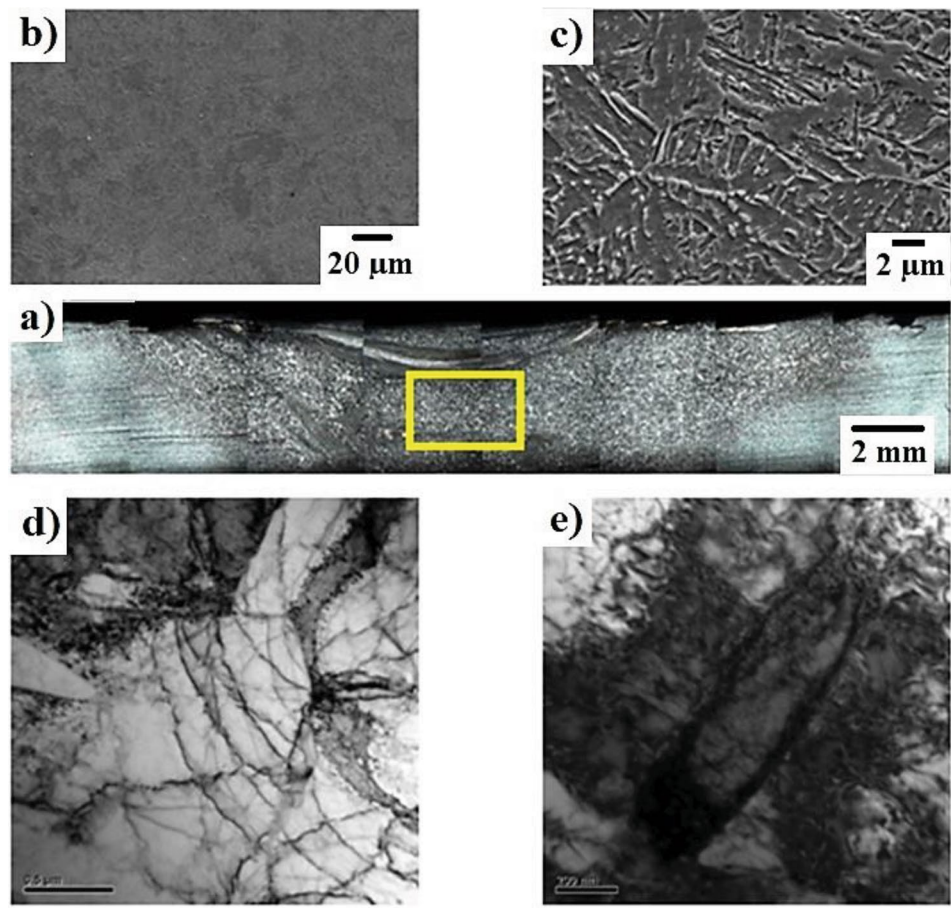
Fig. 12 (**a**) SEM and EDS evaluation of W99 tool pin (**b**) prior to and (**c**) following FSW
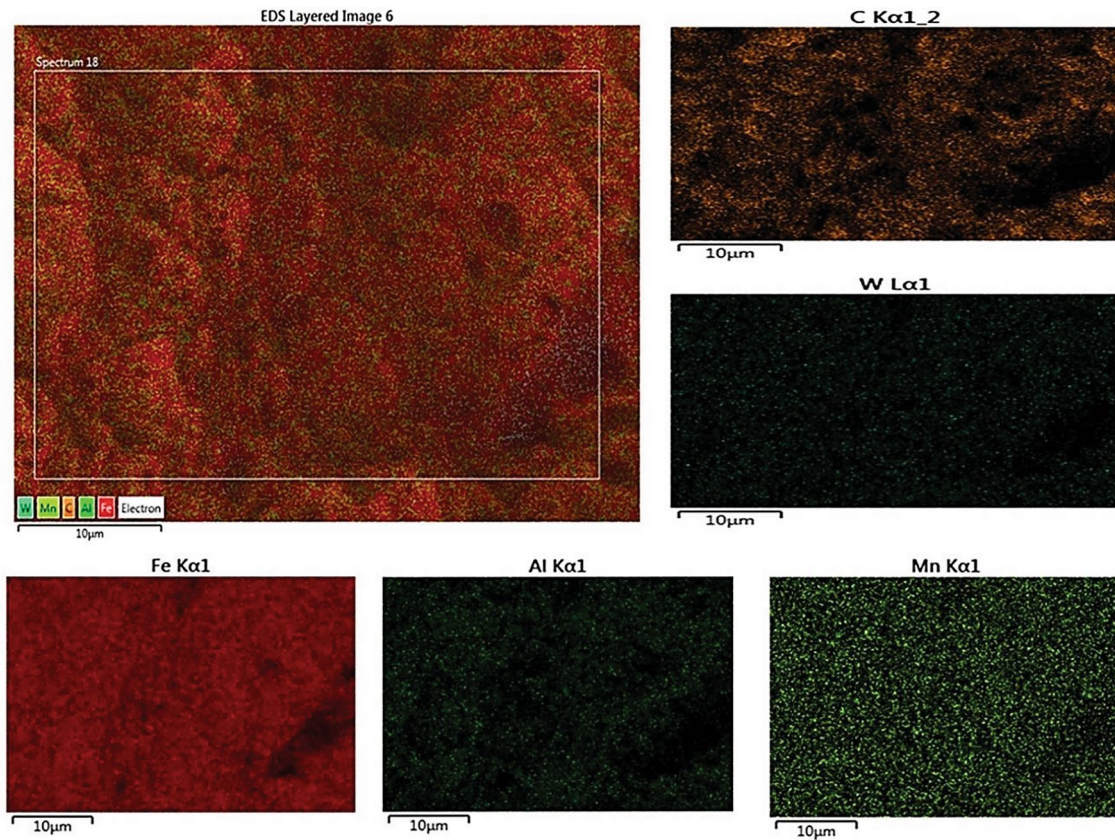
Fig. 13 EDS evaluation of SZ of FSW joint showing no traces of tungsten inclusions

Table 5 Influence of the temperature of preheating on mechanical properties of FSW joints

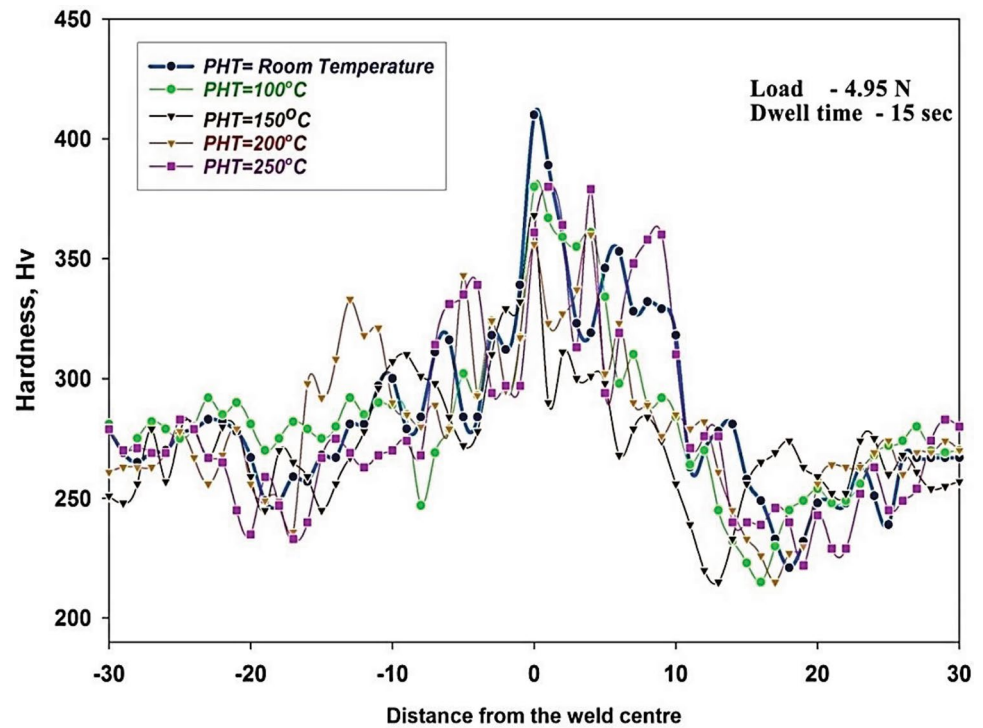| Sr. no.	Preheating temperature, °C	UTS, MPa	0.2% offset YS, MPa	El in a gauge length of 50 mm, %	Failure location	Charpy IT at 25 °C, J
1.	BM	610	540	24	…	62
2.	With no preheating	664	502	19	AS-HAZ	48
3.	100	622	486	22	AS-HAZ	49
4.	150	590	467	19	AS-HAZ	41
5.	200	596	472	18	AS-HAZ	36
6.	250	593	468	16	AS-HAZ	32

make martensite more pronounced, which decreases toughness but does not increase strength [45, 46].

Conclusions

The following results were drawn from this study analyzing the influence of preheating temperature on mechanical properties and microstructure of FSW joints of DMR249A microalloyed steel.

1. The lanthanum oxide-doped tungsten (W99 + 1%La$_2$O$_3$) tool material utilized in this study showed superior stability without requiring dimensional modifications to tool design.
2. The FSW joints produced with no preheating and with preheating at 100 °C displayed greater tensile properties and toughness compared to the FSW joints produced with preheating at 150, 200 and 250 °C. This refers to the greater refinement of SZ microstructure of FSW joints which is made up of greater bainite regions and acicular ferrite.

Fig. 14 Distribution of micro-hardness across the cross section of FSW joints

Table 6 Influence of preheating temperature on mean SZ microhardness of FSW joints

Sr. no.	Preheating temperature, °C	SZ hardness, HV
1.	BM	270
2.	RT	410
3.	100	380
4.	150	368
5.	200	356
6.	250	361

3. Tensile properties and toughness of FSW joints were reduced when the preheating temperature was raised from 100 to 250 °C. This is primarily related to an increased input of heat that results in inclusions of tungsten due to the wear of W99 tool and grain coarsening in SZ of FSW joints.
4. Since the material was stirred using a rotating W99 FSW tool, the finer grain structure evolved in SZ of all the joints, resulting in higher SZ hardness than BM.
5. The SZ hardness of FSW joints decreases with a rise in preheating temperature from 100 to 250 °C. This primarily relates to the increased input of heat that causes growth of grains in SZ microstructure of FSW joints. Due to their lesser hardness than SZ and BM, the majority of the FSW joints on the advancing side HAZ (AS-HAZ) failed.

Declarations

References

1. M. Venkatesh Kannan, N. Arivazhagan, M. Nageswara Rao, G. Madhusudhan Reddy, Effect of inclusions on microstructure and mechanical behavior of multi-pass welded naval grade steel. Proc. Inst. Mech. Eng. Part L: J. Mater. Design Appl. **234**(8), 1071–1083 (2020)
2. G. Chakraborty, R. Rejeesh, S.K. Albert, Study on hydrogen assisted cracking susceptibility of HSLA steel by implant test. Defence Technology. **12**(6), 490–495 (2016)
3. H. Fujii, L. Cui, N. Tsuji, M. Maeda, K. Nakata, K. Nogi, Friction stir welding of carbon steels. Mater. Sci. Eng. A. **429**(1–2), 50–57 (2006)
4. P. Hariprasath, P. Sivaraj, V. Balasubramanian, S. Pilli, K. Sridhar, Assessment of fatigue life prediction on gas metal arc welded DMR249A steel joints for ship hull structure. J. Fail. Anal. Prev. **23**(1), 436–448 (2023)

5. R. Pamnani, G.K. Sharma, S. Mahadevan, T. Jayakumar, M. Vasudevan, B.P.C. Rao, Residual stress studies on arc welding joints of naval steel (DMR-249A). J. Manuf. Process. **20**, 104–111 (2015)

6. R. Pamnani, M. Vasudevan, T. Jayakumar, P. Vasantharaja, Development of activated flux, optimization of welding parameters and characterization of weld joint for DMR-249A shipbuilding steel. Trans. Indian Inst. Met. **70**, 49–57 (2017)

7. R. Mohammed, G.M. Reddy, K.S. Rao, Comparative Studies on microstructure, mechanical and corrosion behaviour of DMR 249A Steel and its welds. Conf. Series Mater. Sci. Eng. **330**(1), 012018 (2018)

8. P. Hariprasath, P. Sivaraj, V. Balasubramanian, S. Pilli, K. Sridhar, Effect of the welding technique on mechanical properties and metallurgical characteristics of the naval grade high strength low alloy steel joints produced by SMAW and GMAW. CIRP J. Manuf. Sci. Technol. **37**, 584–595 (2022)

9. P. Hariprasath, P. Sivaraj, V. Balasubramanian, S. Pilli, K. Sridhar, Effect of welding processes on high cycle fatigue behavior for naval grade HSLA joints: a fatigue strength prediction. Eng. Fail. Anal. **142**, 106783 (2022)

10. M. Venkateshkannan, N. Arivazhagan, M. Nageswara Rao, G. Madhusudhan Reddy, Characterization of weld joints produced by continuous wave and double pulse gas metal arc welding in naval grade high-strength low-alloy steel. Proc. Inst. Mech. Eng. Part E: J. Process Mech. Eng. **237**(5), 1808–1818 (2023)

11. G. Magudeeswaran, V. Balasubramanian, G.M. Reddy, T.S. Balasubramanian, Effect of welding processes and consumables on tensile and impact properties of high strength quenched and tempered steel joints. J. Iron. Steel Res. Int. **15**(6), 87–94 (2008)

12. A. Lambert, A. Lambert, J. Drillet, A.F. Gourgues, T. Sturel, A. Pineau, Microstructure of martensite–austenite constituents in heat affected zones of high strength low alloy steel welds in relation to toughness properties. Sci. Technol. Weld. Joining. **5**(3), 168–173 (2000)

13. R. Pamnani, M. Vasudevan, P. Vasantharaja, T. Jayakumar, Optimization of A-GTAW welding parameters for naval steel (DMR 249 A) by design of experiments approach. Proc. Inst. Mech. Eng. Part L: J. Mater.: Design Appl. **231**(3), 320–331 (2017)

14. P.J. Konkol, M.F. Mruczek, Comparison of friction stir weldments and submerged arc weldments in HSLA-65 steel. Weld. J. **86**(7), 187 (2007)

15. H. Taheri, M. Kilpatrick, M. Norvalls, W.J. Harper, L.W. Koester, T. Bigelow, L.J. Bond, Investigation of nondestructive testing methods for friction stir welding. Metals. **9**(6), 624 (2019)

16. P. Prabhuraj, S. Rajakumar, T. Sonar, M. Ivanov, I. Rajkumar, D.E. Raja, Effect of retrogression and reaging (RRA) on pitting and stress corrosion cracking (SCC) resistance of stir zone of high strength AA7075-T651 alloy joined by friction stir welding. Int. J. Lightweight Mater. Manufact. **6**(2), 264–277 (2023)

17. C. Rajendran, K. Srinivasan, V. Balasubramanian, T. Sonar, H. Balaji, Friction stir welding for manufacturing of a light weight combat aircraft structure. Mater. Testing. **64**(12), 1782–1795 (2022)

18. C. Rajendran, M.V. Kumar, T. Sonar, K. Mallieswaran, Investigating the effect of PWHT on microstructural features and fatigue crack growth behavior of friction stir welded AA2024-T6 aluminum alloy joints. Forces Mech. **8**, 100107 (2022)

19. A. Maciolek, A. Jöckel, S. Völkers, M. Hatzky, T. Suckow, L. Schell, T. Niendorf, Influence of Short-Time Post-Weld heat treatment on the performance of friction stir welded AA7075 aluminum sheets. Int. J. Fatigue. **178**, 107998 (2024)

20. P. Prabhuraj, S. Rajakumar, V. Balasubramanian, T. Sonar, M. Ivanov, D. Elil Raja, Effect of pH value, chloride ion concentration and salt spraying time on salt fog corrosion resistance of friction stir welded AA7075-T651 alloy joints. Int. J. Interact. Des. Manuf. (2023). https://doi.org/10.1007/s12008-023-01415-4

21. T. Sonar, M. Ivanov, E. Trofimov, A. Tingaev, I. Suleymanova, A critical review on solid-state welding of high entropy alloys–processing, microstructural characteristics and mechanical properties of joints. Defence Technol. (2023). https://doi.org/10.1016/j.dt.2023.08.001

22. P. Parasuraman, T. Sonar, S. Rajakumar, Microstructure, tensile properties and fracture toughness of friction stir welded AA7075-T651 aluminium alloy joints. Mater. Testing. **64**(12), 1843–1850 (2022)

23. R.S. Mishra, Z.Y. Ma, Friction stir welding and processing. Mater. Sci. Eng. R. Rep. **50**(1–2), 1–78 (2005)

24. W.M. Thomas, D.G. Staines, I.M. Norris, R. de Frias, Friction stir welding tools and developments. Weld. World. **47**, 10–17 (2003)

25. B. Thompson, S.S. Babu, Tool degradation characterization in the friction stir welding of hard metals. Weld. J. **89**, 256–261 (2010)

26. Y.N. Zhang, X. Cao, S. Larose, P. Wanjara, Review of tools for friction stir welding and processing. Can. Metall. Q. **51**(3), 250–261 (2012)

27. R. Rai, A. De, H.K.D.H. Bhadeshia, T. DebRoy, Friction stir welding tools. Sci. Technol. Weld. Joining. **16**(4), 325–342 (2011)

28. D.G. Mohan, C. Wu, A review on friction stir welding of steels. Chin. J. Mech. Eng. **34**, 1–29 (2021)

29. B. Thompson, Tungsten-based tool material development for the friction stir welding of hard metals. Friction Stir Weld. Proces. VI. **28**, 105–112 (2011)

30. G. Çam, Friction stir welded structural materials: beyond Al-alloys. Int. Mater. Rev. **56**(1), 1–48 (2011)

31. S. Ragu Nathan, V. Balasubramanian, A.G. Rao, T. Sonar, M. Ivanov, K. Suganeswaran, Effect of tool rotational speed on microstructure and mechanical properties of friction stir welded DMR249A high strength low alloy steel butt joints for fabrication of light weight ship building structures. Int. J. Lightweight Mater. Manufact. **6**(4), 469–482 (2023)

32. S. Ragu Nathan, V. Balasubramanian, A. Gourav Rao, T. Sonar, M. Ivanov, C. Rajendran, Influence of tool plunging rate on mechanical properties and microstructure of friction stir welded DMR249A high strength low alloy (HSLA) steel butt joints. Mater. Testing. **65**(10), 1528–1538 (2023)

33. A. Tiwari, P. Pankaj, P. Biswas, A. Kumar, Characterization of ultrafine grain tungsten carbide tool and its wear investigation in friction stir welding of HSLA steel. Tribol. Int. **186**, 108579 (2023)

34. S. Ragu Nathan, V. Balasubramanian, S. Malarvizhi, A.G. Rao, Effect of tool shoulder diameter on stir zone characteristics of friction stir welded HSLA steel joints. Trans. Indian Inst. Met. **69**, 1861–1869 (2016)

35. S.R. Nathan, V. Balasubramanian, S. Malarvizhi, A.G. Rao, An investigation on metallurgical characteristics of tungsten based tool materials used in friction stir welding of naval grade high strength low alloy steels. Int. J. Refract Metal Hard Mater. **56**, 18–26 (2016)

36. W. Gan, Z.T. Li, S. Khurana, Tool materials selection for friction stir welding of L80 steel. Sci. Technol. Weld. Joining. **12**(7), 610–613 (2007)

37. B.B. Mehmet, M. Cemal, The effect of tool rotational and traverse speed on friction stir weldability of AISI 430 ferritic stainless steels. Mater. Des. **33**, 376–383 (2012)

38. S.H.C. Park, Y.S. Sato, H. Kokawa, K. Okamoto, S. Hirano, M. Inagaki, Boride formation induced by pcBN tool wear in friction-stir-welded stainless steels. Metall. Mater. Trans. A. **40**, 625–636 (2009)

39. A. Ozekcin, H.W. Jin, J.Y. Koo, N.V. Bangaru, R. Ayer, G. Vaughn, R. Steel, S. Packer (2004). A microstructural study of

friction stir welded joints of carbon steels. Int J Offshore Polar Eng, 14(04)

40. R. Thamburaj, J.A. Goldak, The influence of preheating temperature on plastic strain distribution during welding. Mater. Sci. Eng. **67**(2), 137–142 (1984)

41. W.M. Thomas, P.L. Threadgill, E.D. Nicholas, Feasibility of friction stir welding steel. Sci. Technol. Weld. Joining. **4**(6), 365–372 (1999)

42. D. Wang, D.R. Ni, B.L. Xiao, Z.Y. Ma, W. Wang, K. Yang, Microstructural evolution and mechanical properties of friction stir welded joint of Fe–Cr–Mn–Mo–N austenite stainless steel. Mater. Des. **64**, 355–359 (2014)

43. X.L. Wan, R. Wei, K.M. Wu, Effect of acicular ferrite formation on grain refinement in the coarse-grained region of heat-affected zone. Mater Charact. **61**(7), 726–731 (2010)

44. K. Yabuuchi, N. Tsuda, A. Kimura, Y. Morisada, H. Fujii, H. Serizawa, A. Hasegawa, T. Nagasaka, Effects of tool rotation speed on the mechanical properties and microstructure of friction stir welded ODS steel. Mater. Sci. Eng. A. **595**, 291–296 (2014)

45. T.J. Lienert, W.L. Stellwag Jr., B.B. Grimmett, R.W. Warke, Friction stir welding studies on mild steel. Weld. J. **89**, 1s–9s (2003)

46. H. Aydin, T.W. Nelson, Microstructure and mechanical properties of hard zone in friction stir welded X80 pipeline steel relative to different heat input. Mater. Sci. Eng. A. **586**, 313–322 (2013)